Modern Physical Chemistry Research (2026)
Clausius Scientific Press, Canada

DOI: 10.23977/mpcr.2026.060101
ISSN 2616-1702 Vol. 6 Num. 1

Multi-Field Coupled Numerical Simulation Study on the Evolution of Semi-Crystalline Polymer Crystals under the Action of Flow Field

Liangzhou Zhang[1,a,*], Yuzhe Cheng[1,b]

[1]*School of Mathematics, Yangzhou University, Yangzhou, 225002, Jiangsu, China*
[a]*laz_liangzhou212@163.com*, [b]*231703103@stu.yzu.edu.cn*
[*]*Corresponding author*

Keywords: Polymer Crystallization; Flow-Induced; Phase-Field Model; Multi-Field Coupling; LB-FV-FD Method

Abstract: This paper constructs a lattice Boltzmann-finite volume-finite difference (LB-FV-FD) multiphysics coupled numerical framework for the flow-induced crystallization process of semi-crystalline polymers, achieving efficient solutions for fluid momentum, latent heat transport, and phase-field interface evolution. The second-order convergence accuracy of the algorithm is verified through static benchmark tests. Furthermore, the evolution of crystals under the flow wake around a cylinder is investigated. The results show that local turbulent shearing and asymmetric diffusion of latent heat break the symmetry of crystal growth from both dynamic and thermodynamic perspectives, inducing severe distortion of the solid-liquid interface along the streamline. The crystal aspect ratio exhibits a nonlinear characteristic of initial sudden increase followed by exponential decay, revealing the dominant role of strong convection in determining mesoscopic morphological distortion, and providing a theoretical basis for optimizing polymer molding processes.

1. Introduction

The macroscopic physical and mechanical properties of semi-crystalline polymers are highly dependent on the microcrystalline structure formed during processing. In actual molding processes such as injection molding and extrusion, polymer melts are usually in a non-isothermal flow state, and the synergistic effect of fluid shear and temperature gradient profoundly affects crystallization kinetics and morphological evolution [1-2] . Phase-field models, by introducing continuously distributed order parameters, can effectively avoid complex interface tracking and show significant advantages in simulating the evolution of polymer crystallization morphology [3]. However, flow-induced crystallization is essentially a strongly coupled "flow-heat-solid" problem involving the release of latent heat of phase change, melt flow deformation, and solid-liquid interface advancement. Traditional single numerical discretization methods often face computational bottlenecks when dealing with such multi-field coupling. The finite difference method (FDM) is difficult to efficiently handle complex fluid dynamic boundaries, while the finite volume method

(FVM) has high computational costs when solving mesoscopic nonlinear phase-field equations. These limitations restrict the application of existing models under complex processing conditions [4-5].

To accurately solve the aforementioned multiphysics coupling problem, this paper constructs a hybrid numerical simulation framework based on Lattice Boltzmann-Finite Volume-Finite Difference (LB-FV-FD). This framework fully leverages the advantages of each discretization method, utilizing LBM to flexibly handle the interaction between complex flow fields and solid boundaries, employing FVM to ensure strict physical conservation of the latent heat source term in the energy equation, and using high-order difference schemes of FDM to solve the nonlinear phase field evolution. Based on this computational framework, this paper focuses on investigating the morphological evolution characteristics of semi-crystalline polymers under multi-field coupling, particularly the intervention mechanism of non-uniform flow fields such as complex flow wakes on the asymmetric growth of crystal nuclei and microstructural transformation , and reveals the kinetic laws of flow-induced polymer crystallization at the mesoscale .

2. Multi-field Coupled Phase-Field Model and LB-FV-FD Numerical Discretization Scheme

2.1. Multiphysics Coupling Control Equations

Polymer flow-induced crystallization involves complex solid-liquid phase transitions, interfacial evolution, and non-isothermal convective transport. To accurately describe this mesoscopic thermodynamic process, this paper introduces a continuous order parameter $\psi(x,t)$ to characterize the local phase states of the system, where $\psi=1$ represents a completely solid crystal and $\psi=0$ represents a pure liquid melt. The microstructure evolution of the system is governed by the total free energy functional F, which is composed of the local chemical free energy density and the interfacial gradient energy.

$$F(\psi, T) = \int_V \left[W\psi^2(1-\psi)^2 + p(\psi)\Delta G(T) + \frac{1}{2}\epsilon^2(\theta)|\nabla\psi|^2 \right] dV \tag{1}$$

In the formula, W is the height of the double-well barrier, and $p(\psi) = \psi^3(10 - 15\psi + 6\psi^2)$ is the monotonic interpolation function that ensures a smooth transition of the extreme points of the potential wells. $\Delta G(T)$ characterizes the thermodynamic phase transition driving force caused by the local temperature deviation from the equilibrium melting point. To accurately characterize the preferred orientation and aspect ratio evolution of polymer crystals on specific crystal planes, an anisotropic gradient energy coefficient $\epsilon(\theta) = \bar{\epsilon}[1 + \delta\cos(k\theta)]$ dependent on the interface normal angle θ is introduced, where δ is the anisotropic intensity and k is the symmetry modulus [6-7] .

After considering the convective transport effects of the macroscopic flow field on the observable phase state, the spatiotemporal evolution of the phase-field interface follows the Ginzburg-Landau equation with convection terms. The dissipative process of the system seeking to minimize total free energy can be described by the following equation:

$$\frac{\partial\psi}{\partial t} + u \cdot \nabla\psi = -M\frac{\delta F}{\delta\psi} \tag{2}$$

In the equation, t represents time, u represents the macroscopic flow field velocity, and M represents the interface mobility. The variational terms on the right side of the equation directly constitute the intrinsic driving force for the development of microscopic crystal nuclei and the evolution of morphological topology. Combined with the shearing and stretching of the external flow field, this equation can spontaneously reproduce the morphological transformation of polymer crystals from symmetrical spherulites to extremely asymmetric cascades. The ordered arrangement of polymer molecular chains is accompanied by significant latent heat release. The accumulation of

local heat will change the temperature gradient of the flow field, and thus dynamically react on the local phase transformation driving force $\Delta G(T)$. Considering the thermal convection and thermal diffusion effects brought about by the non-isothermal flow of the melt, the energy conservation equation of the system is constructed as follows:

$$\frac{\partial T}{\partial t} + u \cdot \nabla T = \alpha \nabla^2 T + \frac{L}{c_p}\frac{\partial \psi}{\partial t} \tag{3}$$

Where T is the local temperature, α is the thermal diffusivity, L is the latent heat of crystallization, and c is the isobaric specific heat capacity. The latent heat source term of phase change on the right side of the equation establishes a strong physical link between the evolution of phase field morphology and the distribution of temperature field at the level of partial differential equations [8].

To enclose the aforementioned thermo-solid coupling system and introduce flow-induced effects, the momentum transfer of the incompressible polymer melt needs to be described by the Navier-Stokes equations. Considering that the continuously growing solid nuclei will exert a strong local resistance to the surrounding melt flow, this paper introduces a fluid resistance penalty term dependent on the order parameter into the momentum equations:

$$\nabla \cdot u = 0 \tag{4}$$

$$\frac{\partial u}{\partial t} + (u \cdot \nabla)u = -\frac{1}{\rho_0}\nabla P + \nu \nabla^2 u + F_{drag}(\psi) \tag{5}$$

In the formula, ρ is the melt density, P is the pressure, and ν is the kinematic viscosity. The construction of the momentum term $F_{drag}(\psi)$ ensures that when the local area approaches the pure solid phase ($\psi \to 1$), the penalty force tends to infinity, forcing the flow velocity inside the crystal nucleus to spontaneously decay to zero, thereby realizing a strict momentum interaction between the flow field and the mesoscopic solid structure in physical space [9-10].

2.2. LB-FV-FD Hybrid Numerical Discretization Scheme

For the aforementioned multiphysics partial differential equation system containing highly nonlinear sources, complex dynamic boundaries, and strict conservation constraints, this paper constructs a hybrid numerical discretization framework of Lattice Boltzmann-Finite Volume-Finite Difference (LB-FV-FD). In solving the phase-field equations, the Lattice Boltzmann method (LBM), with its mesoscopic particle statistical properties, can effectively avoid the numerical dissipation caused by traditional higher-order differences when tracking complex topological side branches. This paper constructs the evolution equation of the single-relaxation time distribution function for the Ginzburg-Landau equations:

$$h_i(x + c_i\Delta t, t + \Delta t) - h_i(x, t) = -\frac{1}{\tau_\psi}\left[h_i(x, t) - h_i^{eq}(x, t)\right] + \Delta t S_i \tag{6}$$

In the formula, τ_ψ is the dimensionless relaxation time, c_i is the discrete velocity spatial component, and S_i is the mesoscopic source term that integrates the thermodynamic phase change driving force and convection effect. The macroscopic order parameter ψ can be obtained directly by summing the distribution function h_i across all discrete directions without explicit geometric interface reconstruction [11].

The local release of latent heat of phase transition in the energy equation imposes extremely stringent requirements on the thermodynamic conservation of the system. To avoid numerical energy drift, this paper employs the finite volume method (FVM) to perform a control volume integral on the temperature equation. By applying the Gaussian divergence theorem to the disjoint

control volumes V and their boundary surfaces A, the partial differential equation is rigorously transformed into a flux equilibrium form on the interface:

$$\int_V \frac{\partial T}{\partial t} dV + \oint_A (uT - \alpha \nabla T) \cdot n dA = \int_V \frac{L}{c_p} \frac{\partial \psi}{\partial t} dV \tag{7}$$

This integral discretization scheme ensures that the convective and conductive heat fluxes across adjacent grid interfaces remain absolutely conserved within any time step, guaranteeing high fidelity in temperature field solutions from the underlying logic of numerical discretization.

The evolution of the macroscopic incompressible flow field is discretized using the finite difference method (FDM). A second-order central difference scheme is used to spatially approximate the convection and viscous terms in the momentum equation, while time-level advancement combined with a projection algorithm decouples pressure and velocity. The introduction of FDM significantly reduces the memory overhead of the overall solution matrix while maintaining high analytical accuracy of the macroscopic flow field.

In the entire multi-field computational framework, the three discretization methods are tightly coupled through explicit data exchange. The macroscopic flow velocity u output by the FDM solution is mapped in real time to the LBM and FVM modules to update convective transport; the local temperature T obtained by the FVM evolution constitutes the supercooling distribution, which is fed back to the mesoscopic source term of the LBM as a thermodynamic driving force; at the same time, the phase field distribution and its phase transition rate updated in real time by the LBM are respectively transformed into the solid phase drag penalty term in the momentum equation and the latent heat release source term in the energy equation, thus completing the numerical closed loop of full coupling of the "thermal-fluid-solid" three fields.

3. Algorithm Validation and Static Crystallization Benchmark Test

3.1 Static isothermal crystallization morphology and kinetic verification

Before introducing the macroscopic non-isothermal flow field, the solution fidelity of the numerical framework under the pure diffusion-reaction mechanism is established. This section selects the static isothermal crystallization process as the first benchmark test example. Under this ideal condition, the fluid convection term disappears (i.e., u=0), and the advancement of the phase field interface is completely dominated by the thermodynamic double potential well and the anisotropic interface energy. An initial micro-nucleus is pre-set at the center of the computational domain, and the system evolution is dominated by the solid-liquid interface dynamics. In Figure 1, under the premise of the set fourfold symmetry modulus (k=4), the initial nucleus spontaneously destabilizes and advances synchronously along four orthogonal preferred directions, forming a characteristic structure with strict geometric symmetry.

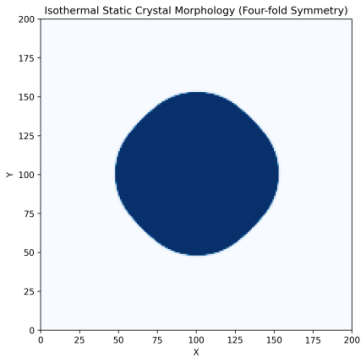

Figure 1. Isothermal Static Crystal Morphology

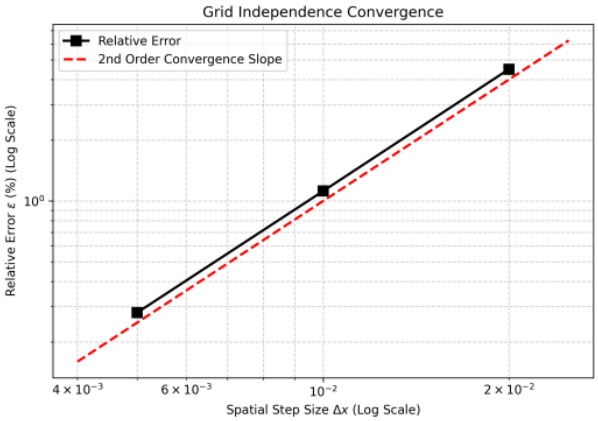

Figure 2. Grid Independence Convergence

3.2 Discrete Scale Independence and Error Convergence Analysis

While maintaining the system's dimensionless geometric scale and constant physical parameters, this section employs multiple spatial grid step sizes Δx with fixed scaling ratios , and strictly follows the Courant-Friedrichs-Lewy (CFL) stability condition to synchronously scale the time step. The following relative error function is defined to quantify the discrete truncation error:

$$\varepsilon = \frac{|\Phi_h - \Phi_{ref}|}{\Phi_{ref}} \times 100\% \tag{8}$$

In the formula, Φ_h is the solid volume fraction obtained by integration at the current test grid resolution, and Φ_{ref} is the reference grid-independent solution obtained by solving with an extremely fine grid.

In Figure 2, the black broken line constructed by the numerical solution maintains an absolute parallel relationship with the red second-order theoretical convergence slope line used as a contrast, proving the independence of the calculation results from the grid density. Furthermore, at the numerical level, it confirms that the spatial center difference scheme used in this paper for discretizing the momentum and phase field equations has achieved the theoretically expected second-order truncation error accuracy $\mathcal{O}(\Delta x^2)$.

4. Polymer Crystallization Characteristics Under the Combined Effects of Flow Around Complex Obstacles and Turbulence

4.1 Strong Coupling Mechanism between the Flow Wake Field and Local Latent Heat Transport

This paper constructs a confined convection model containing a rigid cylindrical obstacle. As shown in Figure 3 , the macroscopic velocity field and streamline topology distribution indicate that after the isothermal polymer melt enters the computational domain from the left at a constant velocity, strong boundary layer separation occurs as it flows through the geometric obstacle. Thanks to the rebound boundary scheme of LBM, the numerical model accurately analyzes the low-velocity backflow region and complex wake vortex structure on the leeward side of the obstacle. Accompanied by the instability of the fluid shear layer, this wake region exhibits significant local turbulence characteristics. This turbulent vortex induced by geometrical abrupt changes completely disrupts the stability and symmetry of the spatial velocity, causing the polymer melt in the wake

region to undergo directional and extremely nonlinear convective pulling, thus providing extreme hydrodynamic boundary conditions for the asymmetric growth of the solid-liquid phase transition interface.

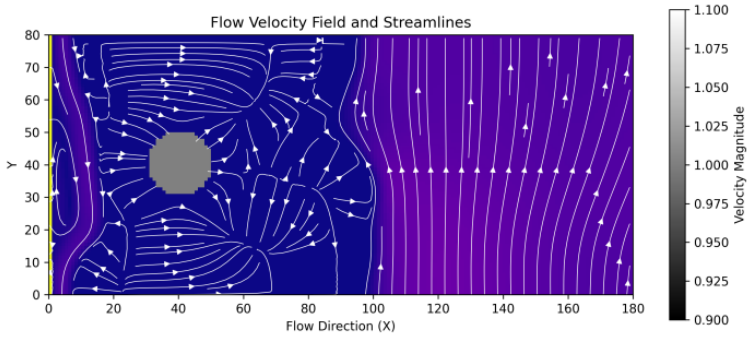

Figure 3. Velocity Field and Streamline Diagram Around the Obstacle

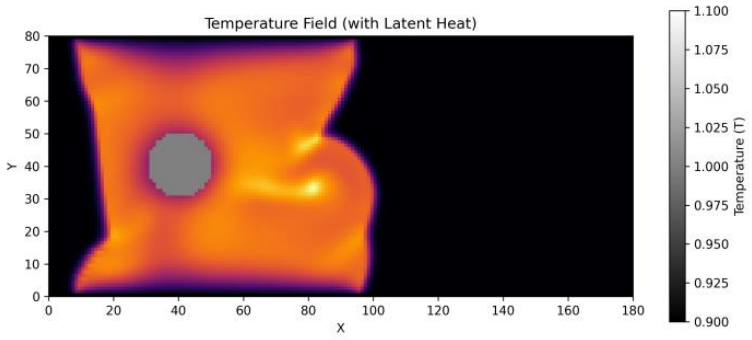

Figure 4. Temperature Field with Latent Heat Release

Driven by a non-uniform turbulent flow field, the thermodynamic state within the system undergoes a dramatic spatiotemporal reconstruction. The temperature field cloud map in Figure 4 visually reveals the strong coupling dynamic interplay between fluid convection transport and the release of latent heat from the solid-liquid phase transition. In the wake region behind the cylindrical obstacle, the ordered crystallization of polymer chains releases considerable latent heat of phase transition to the surrounding melt. The bright color region at the crystallization front (i.e., the local high-temperature extreme region) in the figure is a physical representation of the dramatic release of latent heat. Through rigorous conservation integrals of the energy equation using FVM, the model realistically reproduces the asymmetric diffusion path of this latent heat under the entrainment of turbulent vortices. The non-uniform accumulation of local heat directly weakens the microscopic supercooling ($\Delta T = T_{eq} - T$) in this region, thus forming a strong thermodynamic negative feedback in the evolution of the local phase transition driving force, breaking the symmetry of anisotropic crystal growth from the energy transfer perspective.

4.2 Analysis of Topological Evolution and Morphological Asymmetry of Mesoscopic Crystals

Under the combined influence of the aforementioned turbulent wake and non-uniform temperature field, the growth trajectory of the polymer nuclei exhibits extremely asymmetric distortion characteristics. Figures 5 to 7 fully record the spatiotemporal evolution of the mesoscopic crystal morphology (phase field contour lines) from the early stage (Step = 500), middle stage (Step = 1000), to the late stage (Step = 1500).

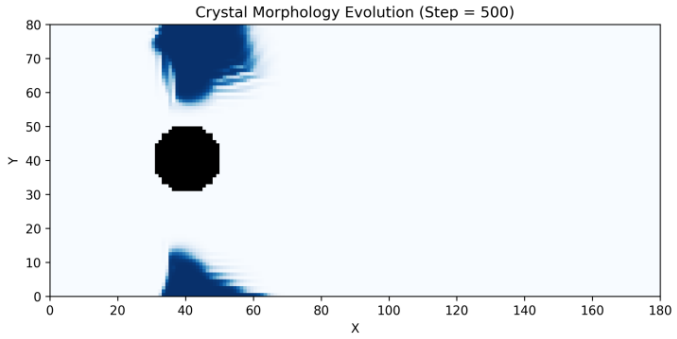

Figure 5. Temporal Evolution of Phase Field Morphology (t=500)

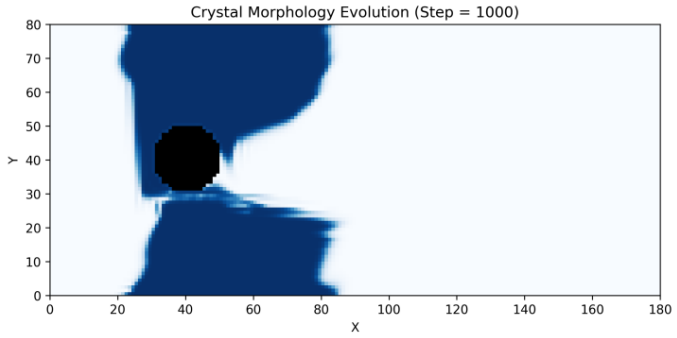

Figure 6. Temporal Evolution of Phase Field Morphology(t=1000)

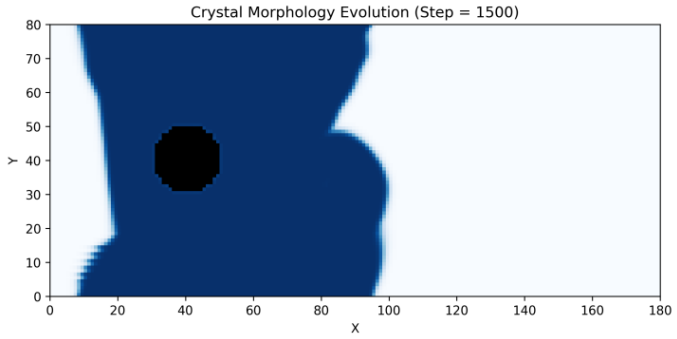

Figure 7. Temporal Evolution of Phase Field Morphology(t=1500)

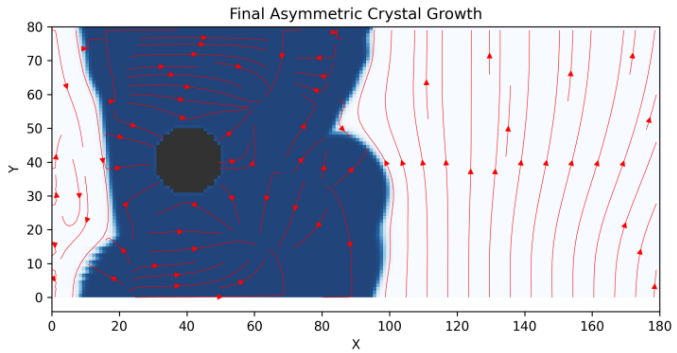

Figure 8. Final Crystal Morphology Superimposed with Streamlines

Figure 8, showing the final morphology and the superimposed diagram of local streamlines, further confirms that the solid-liquid interface of the polymer crystal ultimately achieves a high degree of physical alignment with the local macroscopic streamlines, forming an extremely

irregular spindle-like structure or even a precursor cascade structure. This phenomenon rigorously verifies the decisive role of the convection term $u \cdot \nabla \psi$ in the mesoscopic phase transition dynamics at the partial differential equation level. The physical drag effect of the flow field shear force on the polymer chain segments surpasses the purely thermodynamic interface diffusion mechanism, becoming the core driving force dominating the evolution of microscopic topological morphology.

4.3 Quantitative Dynamic Assessment of Crystal Aspect Ratio Evolution

To strip away visual appearances and quantify the extent to which flow field shear interferes with crystal growth, this paper introduces the crystal aspect ratio (ARR) for transient tracking. Figure 9 shows a quantitative line plot of the crystal ARR versus the evolution time step. In the very early stages of crystallization (around Step=150), the ARR experiences a sudden jump, with a peak value approaching 8.8. This is because when the initial micronuclei are entrained in the high-strain-rate shear layer, the convective pulling rate in the flow direction (X direction) far exceeds the normal growth rate in the vertical flow direction (Y direction).

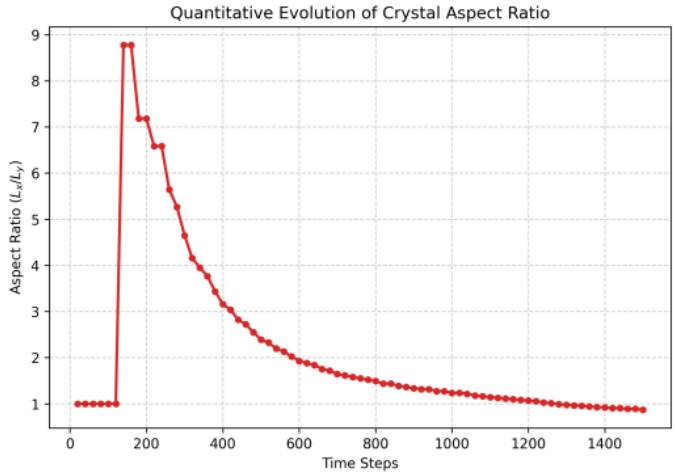

Figure 9. Quantitative Line Graph of Crystal Aspect Ratio as a Function of Evolution Time Step

As the evolution time progresses, the aspect ratio curve exhibits a smooth exponential decay after passing the peak and eventually tends to stabilize (near $L_x/L_y \to 1.0$). When the crystal's coaxial growth gradually approaches the kinetic influence boundary of the computational domain, and the large accumulation of latent heat in the wake region leads to the depletion of coaxial supercooling, restricted lateral (Y direction) growth begins to dominate.

5. Summary

This paper constructs a multiphysics hybrid solution framework based on LB-FV-FD to systematically explore the microscopic topological evolution of semi-crystalline polymers under the synergistic effect of complex flow wakes and latent heat of phase transition. Numerical results show that local turbulence induced by geometrical obstacles and asymmetric diffusion of latent heat break the symmetry of anisotropic crystal growth from both dynamic and thermodynamic dimensions. Under the combined mechanism of fluid drag and restricted thermal conduction, the crystal nucleus irreversibly evolves into an extremely asymmetric spindle structure, whose aspect ratio exhibits a nonlinear characteristic of first abruptly increasing and then exponentially decreasing. This study establishes the core role of convective transport in the dominant microscopic morphological distortion of polymer materials from the mesoscopic partial differential solution level.

Acknowledgement

This work was supported by the College Students' Innovation and Entrepreneurship Training Program of Jiangsu Province (No. 202411117238Y), titled Numerical Simulation of Semi-Crystalline Polymer Crystal Growth Based on LB-FV-FD Method.

References

[1] M. Seki, D.W. Thurman, J.P. Oberhauser et al., Shear-Mediated Crystallization of Isotactic Polypropylene: The Role of Long Chain Long Chain Overlap[J]. Macromolecules, 2002, 35:2583-2594.
[2] J. Su, J. Ouyang, X.D. Wang et al., Lattice Boltzmann method simulation for viscoelas tic flows over a wide range of Weissenberg number[J]. Journal of Non-Newtonian Fluid Mechanics, 2013, 194: 42-59.
[3] Jdvd. Waals, The thermodynamic theory of capillarity under the hypothesis of a continuous variation of density[J]. Journal of Statistical Physics, 1979, 20: 200-244.
[4] L. Gránásy, T. Pusztai, G. Tegze et al., Growth and form of spherulites[J]. Physical Review E, 2005, 72(1): 011605.
[5] Cheung Y, Chow L, Guo Z, et al. LU-net: A Multiscale Probability Search Algorithm for Brain Tumor Segmentation[J]. Journal of Imaging Science and Technology, 2026: 1-10.
[6] X.D. Wang, J. Ouyang, J. Su et al., A phase-field model for simulating various spherulite morphologies of semi-crystalline polymers[J]. Chinese Physics B, 2013, 22(10): 106103.
[7] H.J. Xu, R. Matkar, T. Kyu, Phase-field modeling on morphological landscape of isotactic polystyrene single crystals[J]. Physical Review E, 2005, 72: 011804.
[8] B.X. Yang, C.H. Zhang, F. Wang, A Modified Phase-Field Model for Polymer Crystal Growth[J]. Chinese Journal of Chemical Physics, 2017, 30(5): 538-546.
[9] Y. Rong, H.P. He, W. Cao et al., Multi-scale molding and numerical simulation of the flow-induced crystallization of polymer[J]. Computational Materials Science, 2013, 67: 35-39.
[10] Y. Mu, G.Q. Zhao, A.B. Chen et al., Numerical investigation of the crystallization an dorientation behavior in polymer processing with a two-phase model[J]. Computers and Chemical Engineering, 2014, 63: 91-107.
[11] X.D. Wang, J. Ouyang, W.Zhou et al., A phase field technique for modeling and predicting flow inducedcrystallization morphology of semi-crystalline polymers[J], Polymers, 2016,8(6): 230.